

Photochemical generation of acrylate radicals by sensitizing with acetone–propan-2-ol. A laser photolysis Fourier transform electron paramagnetic resonance study



Annett Beckett,^a Sergej Naumov,^a Reiner Mehnert* and Dieter Beckett^{*b}

^a Institute for Surface Modification, Permoserstraße 15, D-04303 Leipzig, Germany

^b University of Leipzig, Interdisciplinary Group "Time Resolved Spectroscopy", Permoserstr. 15, D-04303 Leipzig, Germany

Received (in Cambridge) 12th March 1999, Accepted 26th April 1999

The sensitized generation of acrylate radicals was studied in acrylate–acetone–propan-2-ol solution by using laser photolysis with time-resolved Fourier transform electron paramagnetic resonance (EPR). In addition to the acetone ketyl radical, vinyl-type radicals of various acrylates were observed in the nanosecond and microsecond time scales. Classification as vinyl-type radical structures was underpinned by quantum-chemical calculations. The acrylate radicals were E/A spin-polarized by the CIDEP radical pair mechanism as described. A triplet exciplex is proposed as the precursor state of the acetone–acrylate radical pair. This interpretation is supported by quantum-chemical calculations.

Introduction

Acrylates are increasingly being used in UV curing and photoresist applications. One of the advantages of the UV curing of acrylates is their high speed of polymerization, which results in monomer conversion in a fraction of a second. The photo-initiated curing of di- and multifunctional acrylates can be regarded as radical polymerization accompanied by cross-linking. In the first step, photons are absorbed by a photo-initiator (or sensitizer), which decomposes into a pair of radicals. One or both of the radicals formed are able to initiate acrylate polymerization. In order to better understand the curing mechanism, it is essential that both the nature of the initiating radicals and their generation mechanism be characterized. In the past, the different reaction steps of the polymerization process have been studied using various experimental methods.^{1–3} In doing so, electron paramagnetic resonance spectroscopy (EPR) proved to be an important tool for studying the structure of primary and secondary radicals. Redox initiators^{2–10} and photolytic radical generating techniques^{11–16} have been used to determine the structure of the initiating and propagating radicals for many different monomers. Besides structural information, time-resolved EPR spectra provide kinetic data on initiation, propagation and termination reactions. Comparable kinetic data can be obtained by pulse radiolysis and laser photolysis experiments with the optical detection of the transients.^{17–20} Although optical detection provides kinetic data at high time resolution, the poor spectral resolution of optical spectroscopy in liquids means that structural information is often scarce. By contrast, well resolved radical spectra can be obtained on a nanosecond time scale using laser photolysis with FT-EPR detection. To elucidate the kinetics of the addition of various initiation radicals to acrylate monomers, EPR experiments with millisecond time resolution have already been performed by Fischer *et al.*^{14–16}

For the present paper, photoinitiated acrylate radical formation was studied using acetone–propan-2-ol as sensitizer. As commonly occurs in the nanosecond and microsecond time scales, the radical kinetics are greatly influenced by the effects of the chemically induced dynamic electron polarization (CIDEP).^{21–24} The nature of the radical precursor state can be elucidated in detail by comparing the predictions of the triplet and radical pair mechanism with the CIDEP pattern observed.

The structure of the primary acrylate radicals and the mechanism of their generation can then be concluded from these results.

Experimental

The laser photolysis experiments were performed with a 308 nm excimer laser produced by Lambda Physik (LPX 105ESC). An energy of 20–50 mJ per pulse and a pulse width of 10 ns were used.

FT-EPR spectra^{24,25} were recorded with an X-band spectrometer we built ourselves²⁶ using a Bruker split-ring module ER 4118 X-MS-5W. The microwave pulse was generated by a fast ECL-PIN diode (rise time 4 ns) and amplified by a 1 kW travelling wave tube amplifier A710/X (LogiMetric, Inc.). The pulse width of the $\pi/2$ microwave pulse was 16 ns. The EPR data were extrapolated into the dead time range (100 ns) by the linear prediction singular value decomposition method (LPSVD),²⁷ which enables spectra with a correct base line and correct intensities to be obtained. The LPSVD program is described elsewhere.²⁸

The acrylates used in these studies were methyl acrylate $\text{CH}_2=\text{CHCOOCH}_3$, butyl acrylate $\text{CH}_2=\text{CHCOOC}_4\text{H}_9$, butyl methacrylate $\text{CH}_2=\text{C}(\text{CH}_3)\text{COOC}_4\text{H}_9$, hexane-1,6-diyl diacrylate $(\text{CH}_2=\text{CHCOOC}_3\text{H}_6)_2$ and acrylic acid $\text{CH}_2=\text{CHCOOH}$. All acrylates and the acrylic acid were purchased from UCB, Speciality Chemicals Division, and were used without further treatment. Spectrograde acetone (99.8%) was purchased from Merck, and the solvent propan-2-ol (99.99%) from Fison. The deuterated compounds d_6 -acetone (99.3%) and d_8 -propan-2-ol (99.7%) were synthesized by DeuChem GmbH.

In order to avoid the accumulation of photolytic reaction products, the degassed solutions flowed through the sample cell (quartz tube with an inner diameter of 2.0 mm) at a rate of approximately 1–2 ml min^{-1} . To prevent oxygen diffusion into the sample solution between the degassing vessel and cavity, the sample flow system was assembled using glass tubing. This system enabled oxygen to be removed down to a concentration of 3×10^{-7} mol dm^{-3} .

Results

Acrylates absorb at 248 nm with typical extinction coefficients

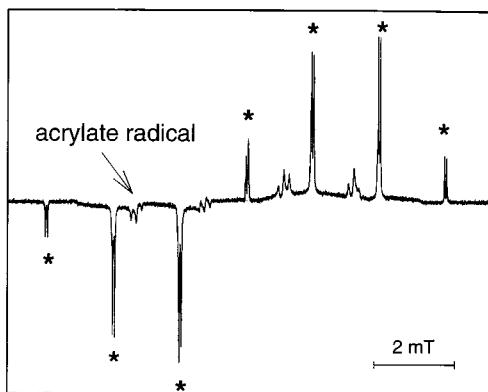


Fig. 1 FT-EPR-spectrum of ketyl radicals (*) and of butyl acrylate radicals generated in an acetone–propan-2-ol mixture (10:90 vol.%) with 0.01 M^{-1} butyl acrylate as solute. Laser energy per pulse: 48 mJ, accumulations per line group: 400; delay time: 1 μs .

in the order of $10^2 \text{ dm}^3 \text{ mol}^{-1} \text{ cm}^{-1}$.²⁹ However, under our experimental conditions, direct excitation of the acrylates in alcoholic solutions by 248 nm laser pulses did not produce a radical concentration which could be detected by time-resolved FT-EPR.

Therefore, various sensitizer systems such as anthraquinone and benzophenone were tested. Only the sensitizer system acetone–propan-2-ol proved useful. The highest EPR signal amplitudes were obtained with a ratio of acetone to propan-2-ol of 1:9. The photoreduction of acetone with propan-2-ol to yield the acetone ketyl radical proceeds as shown in reaction (1).

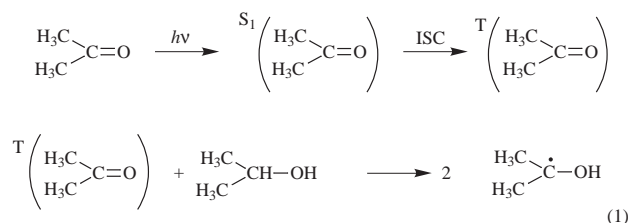


Fig. 1 shows the E/A-spin polarized EPR spectrum of ketyl radicals generated by this sensitizer system. The spectrum was taken at 0.1 μs delay to the laser pulse. The seven line groups (designated by *) were recorded in seven runs with field offsets adjusted to place each line group at the center of Fourier detection. The hyperfine splitting constants tally with the literature values:^{30–34} $a(\text{H}, 2\text{CH}_3) = (1.93 \pm 0.01) \text{ mT}$ and $a(\text{OH}) = (0.06 \pm 0.001) \text{ mT}$. The intensities of the seven-line spectrum show the E/A* pattern as predicted by the CIDEP radical pair mechanism.^{30–34}

Upon adding 0.01 M butyl acrylate to the sensitizer system acetone–propan-2-ol, an additional EPR spectrum with four line groups is observed (see Fig. 1). This EPR spectrum is due to acrylate radicals which are also E/A-spin polarized. This behavior was more pronounced at higher acrylate concentration.

Fig. 2 shows the EPR spectra of the acrylate radicals measured 2 μs after laser excitation in 0.1 M^{-1} butyl acrylate, butyl methacrylate, methyl acrylate, hexane-1,6-diyl diacrylate and acrylic acid solution. At high acrylate concentrations and a delay time of 2 μs , only the EPR spectra of acrylate radicals were detectable.

The spectra of butyl acrylate, methyl acrylate, hexane-1,6-diyl diacrylate and acrylic acid are caused by two unequivalent protons with the additional small splitting of two or three protons, whereas the splitting of butyl methacrylate shows a doublet of triplets. The hfs splitting constants were determined from the simulated spectra shown for butyl acrylate and butyl methacrylate in Fig. 3. The hfs splitting constants and the g factors

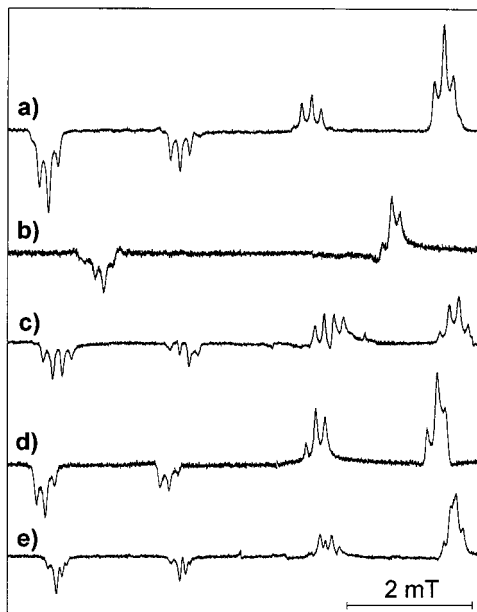


Fig. 2 FT-EPR-spectra of acrylate radicals observed in acetone–propan-2-ol mixtures containing a) butyl acrylate, b) butyl methacrylate, c) methyl acrylate, d) hexane-1,6-diyl acrylate and e) acrylic acid. Acrylate concentration: 0.1 M^{-1} (hexane-1,6-diyl diacrylate: 0.0005 M^{-1}), accumulations per line group: 1000, delay time: 2 μs .

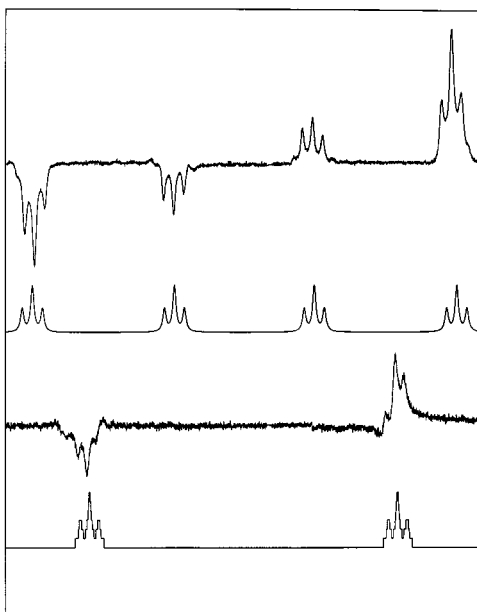


Fig. 3 Comparison of the experimental FT-EPR spectra of butyl acrylate and butyl methacrylate radicals with simulated spectra. The hfs parameters are listed in Table 1.

are listed in Table 1 for all acrylate radicals studied. One important aspect of these results is the high value of the splitting constant of the α -proton with 4.2–4.6 mT, whereas the β -splitting of 2 mT is in the expected region. The small splittings by protons in the γ -position are due to CH_2 -groups in butyl acrylate, butyl methacrylate and hexane-1,6-diyl diacrylate and due to the CH_3 -group in methyl acrylate. The small splitting of each group for acrylic acid is caused by the two different conformers of the acrylic acid radical.⁷

The E/A polarization of the acrylate radicals provides strong evidence that these radicals are generated by the acrylate monomers reacting with the acetone triplet. To test this interpretation the experiments were repeated using deuterated acetone and propan-2-ol. Fig. 4 shows the FT EPR spectra of the $(\text{CH}_3)_2\text{C}^*(\text{OH})$ and $(\text{CD}_3)_2\text{C}^*(\text{OH})$ radicals generated in the partially deuterated system acetone–propan-2-ol (10:90 in

Table 1 Hfs coupling constants a_i , line widths lw and g factors of the acrylate radicals generated by sensitized photoreduction of acetone triplets. The error limits of the g factors given are ± 0.0001

Acrylates	$a_{H\alpha}/mT$	$a_{H\beta}/mT$	a_3/mT	Lw/mT	g factor
Acrylic acid	4.31 ± 0.01	1.99 ± 0.01	0.110 ± 0.005	0.055 ± 0.001	2.0040
Methyl acrylate	4.40 ± 0.01	2.01 ± 0.01	0.148 ± 0.001	0.057 ± 0.001	2.0041
Butyl acrylate	4.22 ± 0.01	2.16 ± 0.01	0.153 ± 0.001	0.060 ± 0.003	2.0048
Butyl methacrylate	4.62 ± 0.01		0.140 ± 0.001	0.060 ± 0.003	2.0048

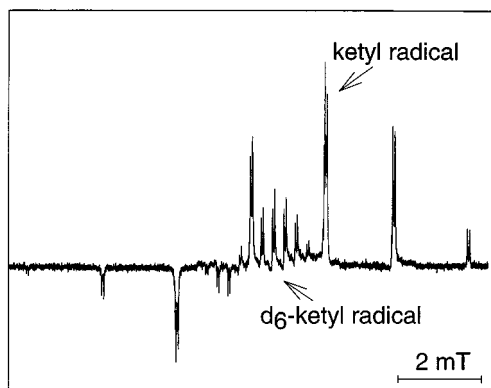


Fig. 4 FT-EPR-spectrum of the protonated and deuterated ketyl radicals generated in a mixture of d_6 -acetone and propan-2-ol. Experimental parameters as in Fig. 1.

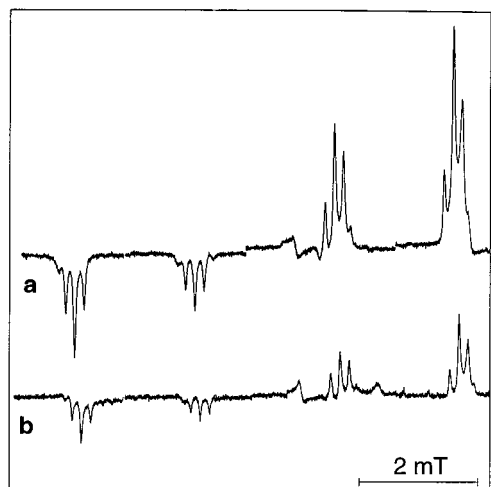


Fig. 5 FT-EPR spectra of butyl acrylate radicals in (a) d_6 -acetone-propan-2-ol and (b) acetone- d_8 -propan-2-ol. [butyl acrylate] = 0.1 M, other parameters as in Fig. 1.

vol%). Coupling constants, g factors and the E/A polarization pattern correspond to those contained in ref. 34. After adding 0.1 M butyl acrylate to the partially deuterated solvent mixture, the EPR spectra given in Fig. 5a (solvent d_6 -acetone-propan-2-ol) and 5b (solvent acetone- d_8 -propan-2-ol) were observed. These spectra are nearly identical and no additional EPR lines were detected. The hfs coupling constants deviate slightly from those measured in protonated solutions (*cf.* Table 1): $a_1(H_\alpha) = (4.36 \pm 0.01)$ mT, $a_2(H_\beta) = (2.01 \pm 0.01)$ mT and $a_3(OCH_2) = (0.154 \pm 0.001)$ mT. The g factors were determined as $g = 2.00491$ (d_6 -acetone-propan-2-ol) and $g = 2.00494$ (acetone- d_8 -propan-2-ol). These results indicate that the primary reaction of acetone radical formation ought to be the reaction of the acetone triplet with the acrylate monomer rather than hydrogen transfer from the solvent or an additional reaction by a solvent radical.

By varying the time delay between the laser pulse and the microwave detection pulse, the kinetics of the ketyl radical decay were followed at the first high field and low field hfs lines ($m_1 = \pm 1$) with butyl acrylate as scavenger (Fig. 6). The inten-

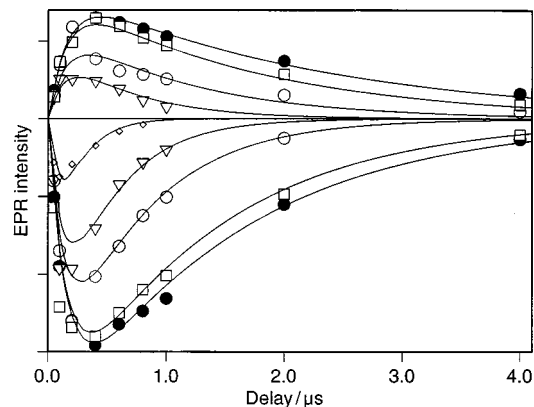
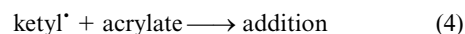
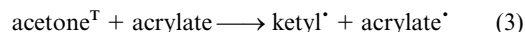
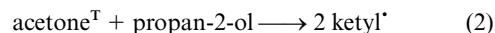


Fig. 6 Time dependence of the EPR intensities of the first low and high field line group of the ketyl radicals at different butyl acrylate concentrations. Sample: ●: acetone-propan-2-ol with butyl acrylate: □: 0.005 M, ○: 0.01 M, ▽: 0.03 M and ◇: 0.1 M.

sities were determined by integrating the two line groups. The concentration of butyl acrylate was varied in the range of (0.005–0.1) M. In order to describe the EPR intensities as a function of time, the reactions (2)–(5) were used.

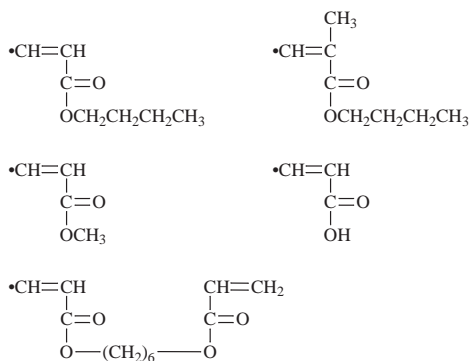


By fitting the ketyl radical time profiles depending on the butyl acrylate concentration, the rate constants k_1 and k_2 were estimated as $k_1 = 8.6 \times 10^6 \text{ M}^{-1} \text{ s}^{-1}$ and $k_2 = 1.5 \times 10^8 \text{ M}^{-1} \text{ s}^{-1}$. Our value of the rate constant k_1 is of the same order of magnitude as that determined by Fischer,³⁵ who gives $k_1 = 2.0 \times 10^6 \text{ M}^{-1} \text{ s}^{-1}$. The rate constant k_1 controls the rise time of the ketyl EPR signal in neat solvent, whereas in acrylate solution the yield of the ketyl radical is determined by competition between reactions (2) and (3). Furthermore, reaction (4) is determined by the decay time constant of the ketyl radicals. These decay processes can be described by a rate constant $k_3 = 5.2 \times 10^7 \text{ M}^{-1} \text{ s}^{-1}$. In the time range shown, radical recombination (reaction (5)) can be neglected at higher acrylate concentrations. The signal rise of the acrylate radicals is only controlled by reaction (3), because the radicals generated by reaction (3) are spin-polarized with a higher intensity than the radicals generated by reaction (4). Reaction (4) eliminates the radical pair polarization, and because of the low amount of net polarization, the EPR signal of this acrylate radical only contributes a small part to the spectra measured. This part cannot be separated in the experiments described here.

Discussion

The hfs parameters of the acrylate radicals studied are listed in Table 1. From the coupling of two nonequivalent protons for butyl acrylate, methyl acrylate, acrylic acid and hexane-1,6-diyl

diacrylate and the coupling of one proton for butyl methacrylate, we conclude that the acrylate radicals are of vinyl-type.



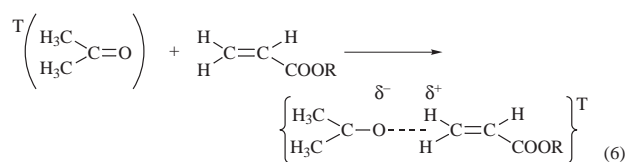
The large coupling constant is attributed to the proton in the α -position and the medium coupling constant to that in the β -position. There are few reports concerning the hfs coupling constants of vinyl radicals in the literature.^{36–38} Fessenden³⁸ observed coupling constants of 1.34 mT and 3.7/6.5 mT for the vinyl radical $\text{CH}_2=\dot{\text{C}}\text{H}^\cdot$, where the large values were assigned to the β -protons. Our assumption that the splitting of 4.2 mT is assigned to an α -proton splitting is supported by the comparison between the spectra of butyl acrylate and butyl methacrylate (*cf.* Fig. 2). Therefore we assign the 4.2 mT coupling constant to the α -proton. The small splitting (three or four lines) in each group is due to the ester group with two δ -protons (butyl acrylate, butyl methacrylate and hexane-1,6-diyldiacrylate) or with three δ -protons (methyl acrylate). The small splitting into four lines for acrylic acid is caused by the two different conformers of the acrylic acid.⁷ The absence of the hfs splitting from the methyl group in butyl methacrylate can be interpreted by their fast free rotation. From a coupling constant of $a(\text{CH}_3) \cong 2.0$ mT and assuming fast exchange we estimate an upper limit of the rotational correlation time of $\tau_{\text{rot}} \ll 2.8$ ns. The g values listed in Table 1 are in agreement with the data obtained by Kasai³⁶ and Ozawa and Kwan³⁷ for similar vinyl-type radicals.

In order to test the classification of the radical structures observed as vinyl-type radicals, quantum-chemical calculations were performed using the standard version of the PM3 method³⁹ from HYPERCHEM 5.01 for Windows. Geometry optimization of the open shell molecular systems was performed in a vacuum using the Polac–Ribiere conjugate gradient method in the unrestricted Hartree–Fock (UHF) formalism. To compare molecular binding energies and to compute the electronic transition energies of radicals, half electron restricted open shell Hartree–Fock (ROHF) calculations were performed for the optimized structure in UHF.

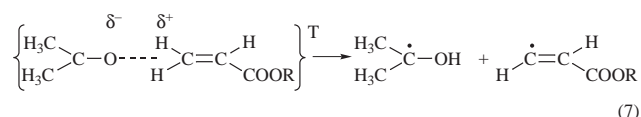
The optimization of the radical geometry by the UHF method results in a planar structure for the butyl acrylate radicals with all C atoms located in a plane. This structure belongs to the C_s symmetry point group. The ester group with the first CH_2 group is bent towards the unpaired electron. The through space distance between C_1 and the two H atoms of the first CH_2 group was found to be 0.26 nm. This distance is comparable to the distance of the unpaired electron in a carbon–carbon chain with protons in the γ position. This corresponds with the coupling constants obtained for the ester protons in the acrylate radicals (*cf.* Table 1). For the butyl methacrylate radical, geometry optimization results in a nonplanar conformation with an asymmetric radical structure, where the two vinyl carbon atoms and the methyl group are located in a plane. Because of the fast rotation of the methyl group, the EPR spectrum of the butyl methacrylate radical cannot provide more structural information. The interpretation of an acrylate radical structure exhibiting an unpaired electron at the C_1 -position is supported by the results of pulse radiolysis experiments.²⁹ In pulse radiolysis

experiments on acrylates with optical detection, the radical cation was directly detected, which deprotonates to generate vinyl-type radicals. In air-saturated solutions an absorption band attributed to vinyl-peroxy radicals was observed at 391 nm. Quantum-chemical calculation of the optical spectra of different vinyl-peroxy radicals suggests that the C_1 -vinyl-peroxy radicals ought to show optical absorption in the range 390–410 nm, whereas the C_2 -vinyl-peroxy radicals ought to absorb at about 350 nm. From these results it can be concluded that the acrylate radical cation deprotonates at the C_1 -position. The UV-visible electronic spectra of vinyl-peroxy radicals were calculated using the ROHF option at the single excitation (SCI) level of the configuration interaction wave function and the energy criterion, while the configuration interaction method for calculating the UV-visible electronic spectra is only available for ROHF.

The E/A spin-polarized acrylate radical spectra indicate that the dominating mechanism of the acrylate radical generation is the direct interaction of the acrylate with the acetone triplet. A radical transfer process cancels the primary E/A radical pair polarization. Only a net polarization is transferred to the secondary radical. This means that the polarization pattern observed for the acrylate radicals enables conclusions concerning the primary reaction step of the photosensitized acrylate radical generation. Both the E/A polarization pattern and the value of the rate constant measured $k_2 = 1.5 \times 10^8 \text{ M}^{-1} \text{ s}^{-1}$ are in accordance with the assumption that an intermediate triplet exciplex is formed (reaction (6)). Quantum-chemical



calculations suggest that a triplet exciplex is formed with a distance of 0.14 nm between the carbonyl oxygen and C_1 at the double bond, and the negative charge is shifted to acetone. This charge separation forms the driving force for a subsequent proton transfer. As a result the radical pair shown in equation (7) is generated.



Conclusions

The photoreduction of acetone triplets by acrylate monomers generates acetone ketyl radicals and acrylate vinyl-type radicals. It is suggested that an intermediate triplet exciplex is generated as the precursor of the primary ketyl–acrylate radical pair. A rate constant of $5.2 \times 10^7 \text{ M}^{-1} \text{ s}^{-1}$ was estimated for the reaction of ketyl radicals with butyl acrylate.

Acknowledgements

We would like to express our gratitude for the financial support generously granted by the Deutsche Forschungsgemeinschaft. Our thanks are also extended to Dr W. Knolle for fruitful discussions.

References

- 1 G. Moad and D. H. Solomon, *The Chemistry of Free Radical Polymerization*, Pergamon Press, Oxford, 1995.
- 2 J. Kochi (Ed.), *Free Radicals*, Wiley Interscience, New York, 1972 and references therein.

- 3 D. J. T. Hill, J. H. O'Donnell and P. J. Pomery, *Electron Spin Reson.*, 1992, **13A**, 202 and references therein.
- 4 H. Fischer, *Z. Naturforsch., Teil A*, 1964, **19**, 866.
- 5 H. Fischer, *Adv. Polym. Sci.*, 1968, **5**, 463.
- 6 J. Hellebrand and P. Wünsche, PhD Thesis, Leipzig, 1974.
- 7 B. C. Gilbert, J. K. Stell and M. Jeff, *J. Chem. Soc., Perkin Trans. 2*, 1988, 1867.
- 8 B. C. Gilbert, J. R. L. Smith, E. C. Milne, A. C. Whitwood and P. Taylor, *J. Chem. Soc., Perkin Trans. 2*, 1993, 2025.
- 9 B. C. Gilbert, J. R. L. Smith, E. C. Milne, A. C. Whitwood and P. Taylor, *J. Chem. Soc., Perkin Trans. 2*, 1994, 1759.
- 10 A. Matsumoto and B. Giese, *Macromolecules*, 1996, **29**, 3758 and references therein.
- 11 W. Lung-min and H. Fischer, *Helv. Chim. Acta*, 1983, **66**, 138.
- 12 K. Münger and H. Fischer, *Int. J. Chem. Kinet.*, 1985, **17**, 809.
- 13 H. Fischer and H. Paul, *Acc. Chem. Res.*, 1987, **20**, 200.
- 14 A. Salikhov and H. Fischer, *Appl. Magn. Reson.*, 1993, **5**, 445.
- 15 K. Heberger and H. Fischer, *Int. J. Chem. Kinet.*, 1993, **25**, 249 and 913.
- 16 J. Q. Wu and H. Fischer, *Int. J. Chem. Kinet.*, 1995, **27**, 167.
- 17 J. Schmidt and U. Decker, *Proc. Tihany Symp. Radiat. Chem.*, eds. J. Dobo and R. Schiller, Akademiai Kiado, Budapest, 1991, p. 239.
- 18 L. Wojnarovits, E. Takacs, J. Dobo and G. Földiák, *Radiat. Phys. Chem.*, 1992, **39**, 59.
- 19 R. Mehnert and W. Knolle, *Radiat. Phys. Chem.*, 1995, **46**, 963.
- 20 W. Knolle and R. Mehnert, *Nucl. Instrum. Methods Phys. Rev., Sect. B*, 1995, **105**, 154.
- 21 L. T. Muus, P. W. Atkins, K. A. McLauchlan and J. B. Pedersen (Eds.), *Chemically Induced Magnetic Polarization*, Reidel, Dordrecht, 1977.
- 22 K. A. McLauchlan, in *Modern Pulsed and Continuous-Wave Electron Spin Resonance*, ed. L. Kevan and M. K. Bowman, Wiley Interscience, New York, 1990, p. 285.
- 23 K. A. McLauchlan, *J. Chem. Soc., Perkin Trans. 2*, 1997, 2465.
- 24 M. K. Bowman, in *Modern Pulsed and Continuous-Wave Electron Spin Resonance*, ed. L. Kevan and M. K. Bowman, Wiley Interscience, New York, 1990, p. 1.
- 25 H. van Willigen, P. R. Levstein and M. H. Ebersole, *Chem. Rev.*, 1993, **93**, 173.
- 26 T. Kausche, J. Säuberlich, E. Trobitzsch, D. Beckert and K.-P. Dinse, *Chem. Phys.*, 1996, **208**, 375.
- 27 D. S. Stephenson, *Prog. Nucl. Magn. Reson. Spectrosc.*, 1988, **20**, 515.
- 28 J. Säuberlich, PhD Thesis, Leipzig, 1996.
- 29 W. Knolle, personal communication.
- 30 S. K. Wong, T.-M. Chiu and J. R. Bolton, *J. Phys. Chem.*, 1981, **85**, 12.
- 31 K. A. McLauchlan and D. G. Stevens, *J. Magn. Reson.*, 1985, **63**, 473.
- 32 M. C. Thurnauer, T.-M. Chiu and A. D. Trifunac, *Chem. Phys. Lett.*, 1985, **116**, 543.
- 33 K. Tominaga, S. Yamauchi and N. Hirota, *J. Chem. Phys.*, 1990, **92**, 5175 and references therein.
- 34 P. R. Levstein and H. van Willigen, *J. Chem. Phys.*, 1991, **95**, 900.
- 35 B. Blank, A. Henne, G. P. Laroff and H. Fischer, *Pure Appl. Chem.*, 1975, **41**, 475.
- 36 P. H. Kasai, *J. Phys. Chem.*, 1982, **86**, 4096.
- 37 T. Ozawa and T. Kwan, *J. Chem. Soc., Chem. Commun.*, 1983, 80.
- 38 R. W. Fessenden and R. H. Schuler, in *Advances in Radiation Chemistry 2, 1*, ed. M. Burton and J. L. Magee, Wiley-Interscience, New York, 1969.
- 39 HYPERCHEM, Rel. 3; *Computational Chemistry*, Autodesk, Inc., 1992.

Paper 9/01975H